Recent Advances in Computational Mechanics – Łodygowski, Rakowski & Litewka (Eds)
© 2014 Taylor & Francis Group, London, ISBN 978-1-138-02482-3

Corrected shape functions for six-node triangular element for heat conduction

P. Jarzębski & K. Wiśniewski
Institute of Fundamental Technological Research, Polish Academy of Sciences, Warsaw, Poland

ABSTRACT: In this paper, we derived the corrected shape functions for 6-node triangular element using the concept proposed in (Celia & Gray 1984). These shape functions were implemented in the two-dimensional 6-node triangular element for heat conduction as a replacement of the isoparametric ones. The numerical tests indicate that, for distorted meshes, the new element is more accurate than the standard element. Comparisons of the accuracy of a range of triangular and quadrilateral elements also are provided.

1 INTRODUCTION

The corrected shape functions were proposed in (Celia & Gray 1984) as a generalization of the standard concept of isoparametric elements. They were derived and tested for an 8-node (serendipity) quadrilateral element for the heat conduction equation integrated by the 4×4 rule.

The corrected shape functions have been proven useful also in plane elasticity problems solved by 9-node elements based on two-level interpolations of strain (AS and MITC elements). It was shown in (Wisniewski & Panasz 2013) that, besides the modified transformations, the corrected shape function were one of the essential improvements of the MITC9 element, which enabled passing the patch test for some irregular meshes. In (Panasz, Wisniewski, & Turska 2013), it was shown that several well known formulations of nine-node elements for plane elasticity can benefit from using the corrected shape functions.

In the current paper, we extend the range of applications of the concept of the corrected shape functions of (Celia & Gray 1984) to the six-node triangular element for heat conduction, which requires

1. generalization of the concept of the corrected shape functions to the six-node triangular element, which is formulated in terms of the area (barycentric) coordinates. This is not so natural as in the case of quadrilaterals, for which the natural coordinates are used.
2. implementation of the corrected shape functions in the six-node element and passing it through a range of tests involving several types of mesh distortions. The purpose is to confirm passing the patch test, and to show their improved accuracy and reduced sensitivity to mesh distortions.

2 CORRECTED SHAPE FUNCTIONS

2.1 *Corrected shape functions for one dimensional element*

Let us first present the corrected shape functions for a one-dimensional three-node element. The standard isoparametric shape functions of such an element are

$$\mathbf{N}_\xi \doteq [(1-\xi)(1-2\xi),\ 4(1-\xi)\xi,\ \xi(2\xi-1)], \quad (1)$$

where the coordinate $\xi \in [0, 1]$. If in derivation of these functions a parameter α is used as a coordinate of the middle node instead of zero, then we obtain the corrected shape functions

$$\tilde{\mathbf{N}}_\xi \doteq \left[\frac{(1-\xi)(1-2\xi+2\alpha)}{1+2\alpha},\ \frac{4(1-\xi)\xi}{1-4\alpha^2},\ \frac{\xi(2\xi-2\alpha-1)}{1-2\alpha}\right], \quad (2)$$

where the parameter $\alpha \in (-\frac{1}{2}, +\frac{1}{2})$ describes the position of the middle node in the natural coordinates. In other words, α is a shift of the middle node from $\xi = \frac{1}{2}$, and it can be calculated using distances of nodes in the physical space. For $\alpha = 0$, the corrected shape functions reduce to the standard ones.

2.2 *Standard shape functions for six-node element*

The standard shape functions for the six-node element are as follows:

$$\begin{aligned} &N_1(\xi,\eta) \doteq \xi(\xi-\zeta-\eta),\ N_2(\xi,\eta) \doteq \eta(\eta-\xi-\zeta),\\ &N_3(\xi,\eta) \doteq \zeta(\zeta-\eta-\xi),\ N_4(\xi,\eta) \doteq 4\xi\eta, \quad (3)\\ &N_5(\xi,\eta) \doteq 4\eta\zeta, \qquad N_6(\xi,\eta) \doteq 4\xi\zeta, \end{aligned}$$

where $\zeta \doteq 1-\xi-\eta$ and the area (barycentric) coordinates $\xi, \eta, \zeta \in [0, 1]$. The nodes are numbered as shown

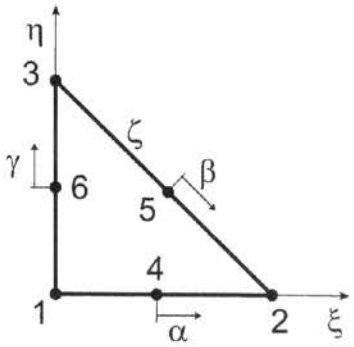

Figure 1. Six-node element. Numbering of nodes and positive values of distortion parameters α, β, γ.

in Fig. 1, where 1, 2, 3 are the corner nodes, and 4, 5, 6 designate the side nodes.

2.3 *Corrected shape functions for six-node element*

For the six-node element, the shifts of the side nodes are described by 3 scalar parameters, $\alpha, \beta, \gamma \in (-\frac{1}{2}, +\frac{1}{2})$, see Fig.1. The corrected shape functions of the 6-node element (obtained in an analogous way to these for the one-dimensional element) are defined as follows:

$$\begin{aligned}
\bar{N}_1 &\doteq \frac{\xi[(2\gamma+1)(1-2\alpha)\xi-(2\alpha-1)(2\gamma-1)\zeta-(2\gamma+1)(2\alpha+1)\eta]}{(2\gamma+1)(1-2\alpha)},\\
\bar{N}_2 &\doteq \frac{\eta[(1-2\beta)(2\alpha+1)\eta-(2\beta-1)(2\alpha-1)\xi-(2\alpha+1)(2\beta+1)\zeta]}{(2\alpha+1)(1-2\beta)},\\
\bar{N}_3 &\doteq \frac{\zeta[(2\beta+1)(1-2\gamma)\zeta-(2\beta-1)(2\gamma-1)\eta-(2\beta+1)(2\gamma+1)\xi]}{(2\beta+1)(1-2\gamma)},\\
\bar{N}_4 &\doteq \frac{4\xi\eta}{1-4\alpha^2}, \qquad \bar{N}_5 \doteq \frac{4\eta\zeta}{1-4\beta^2}, \qquad \bar{N}_6 \doteq \frac{4\xi\zeta}{1-4\gamma^2}.
\end{aligned} \tag{4}$$

When the parameters α, β, γ are set to zero then the standard shape functions of eq. (3) are recovered.

The procedure of determining α, β, γ is as follows. Let us determine α for the side curve 1-4-2 given in the parametric form $X(\xi) = \overline{\mathbf{N}}_\xi \cdot [X_1, X_4, X_2]$ and $Y(\xi) = \overline{\mathbf{N}}_\xi \cdot [Y_1, Y_4, Y_2]$, where $\overline{\mathbf{N}}_\xi$ is defined in eq. (2). The fractional distance of node 4 relative to nodes 1 and 2 (along the boundary curve) is required to be identical in the physical space and in the local space,

$$\frac{L_0^{1/2+\alpha}}{L_0^1} = \frac{\int_0^{1/2+\alpha} d\xi}{\int_0^1 d\xi}, \tag{5}$$

where the arc-length of the curve in the physical space is

$$L_0^A \doteq \int_0^A \sqrt{(dX/d\xi)^2 + (dY/d\xi)^2}\, d\xi, \tag{6}$$

and $A \in [0, 1]$. Eq. (5) can be transformed to a single non-linear equation in α and solved using e.g. the Newton method. The initial value of α is selected as described in (Wisniewski & Panasz 2013).

3 NUMERICAL TESTS

In this section, we present numerical tests of the two-dimensional 6-node triangular element for the heat conduction equation, in which the corrected shape functions described in Sect. 2 are implemented. The tested triangular elements are designated as follows:

1. "6" – 6-node, standard quadratic shape functions, 3-point Gauss integration,
2. "6c" – 6-node, corrected quadratic shape functions, 3-point Gauss integration,
3. "3" – 3-node, standard linear shape functions, 1-point Gauss integration.

The new element is designated by "6c". For reference, we also use the triangular elements of ABAQUS (Simulia 2010) and FEAP (Taylor 2010). The mesh for 3-node elements is obtained by dividing each 6-node element into four 3-node elements and uses the same nodes. Note that four "3" elements use more Gauss points than one "6" or "6c" element!

Besides, we provide results obtained by the quadrilateral elements for the heat conduction equation:

1. "8CG" and "8CGc" – the 8-node quadrilateral elements of (Celia & Gray 1984), which are based either on the standard or the corrected quadratic shape functions, respectively. 4×4 Gauss integration.
2. "8" and "8c" – our implementation of the above described elements "8CG" and "8CGc" but written in double precision instead of the single precision used in the cited paper.
3. "9" and "9c" – our 9-node quadrilateral elements, which are based either on the standard shape functions or the corrected shape functions, respectively. 3×3 Gauss integration.
4. "4" – our bilinear 4-node quadrilateral element. 2×2 Gauss integration.

Note that the elements based on the corrected shape functions are designated by the appended "c".

We tacitly assume that any consistent set of units can be used for the data in the numerical examples. In all tests, the thickness $h = 1$.

3.1 *Eigenvalues of single element*

The eigenvalues of a tangent matrix of a single element are checked. The boundary conditions are not imposed and the thermal conductivity $k = 10$ is used.

Two geometries are considered: (1) the equilateral triangle with regularly placed side nodes, and (2) the irregular shape obtained by shifting the vertex A of the triangle by the vector $d = [0.25, 0.25]$, which implies different element's shapes for the standard and the corrected shape functions, see Fig. 2.

All the tested elements have a correct number of zero eigenvalues (1) for the standard and the corrected shape functions.

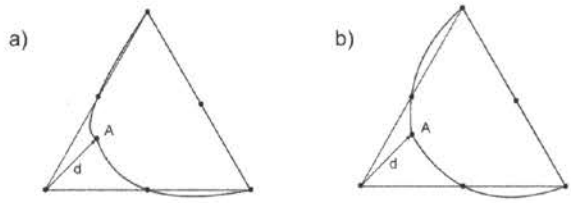

Figure 2. Eigenvalues of single element. The same coordinates of nodes imply different shapes of the element for: a) standard shape functions, b) corrected shape functions.

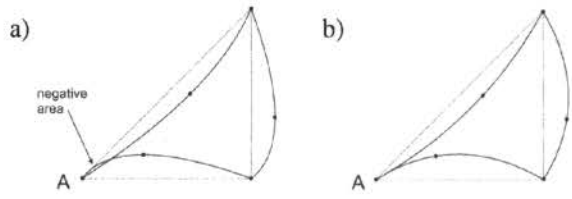

Figure 3. Eigenvalues of single element. Shapes of distorted element with coordinates specified by eq. (7): a) standard shape functions, b) corrected shape functions.

Remark. We have checked that the 3-point Gauss integration does not yield negative eigenvalues regardless of the positions of nodes, neither for the standard nor the corrected shape functions. However, the 6-point integration and the standard shape functions, which are used e.g. by the DC2D6 element of ABAQUS, yield a negative eigenvalue, for instance, for the nodes shown in Fig. 3, and having the following coordinates:

$$\{(0,0),\ (10,0),\ (10,10),\ (3.6,1.4),\ (11.4,3.6),\ (6.4,5)\}, \quad (7)$$

We see that a negative area at the vertex A appears for the standard shape functions but not for the corrected ones. Clearly, the elimination of the negative area removes the negative eigenvalue. The 7-point integration rule, which is used e.g. by FEAP, also does not yield a negative eigenvalue in this case.

3.2 *Patch test*

The concept of a patch test was proposed by (Irons 1966) and it is remains of crucial importance for finite elements, see (Zienkiewicz, Taylor, & Zhu 2005, p. 329). For heat conduction elements, it verifies that a patch of irregular elements is able to reproduce exactly the linear temperature field. We used the ten-element patch shown in Fig. 4; the same patch is used e.g. in ABAQUS (Simulia 2010). The temperature field is defined in two ways:

1. Linear temperature field in two directions,

$$T(x,y) \doteq 200x + 100y. \quad (8)$$

2. Parabolic temperature field in one direction,

$$T(x) \doteq 200x + \frac{25}{9}x(6-25x), \quad (9)$$

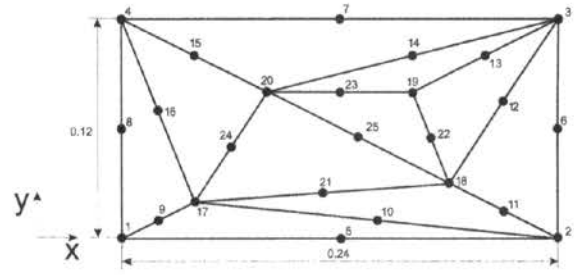

Figure 4. Ten-element patch test. Non-distorted mesh.

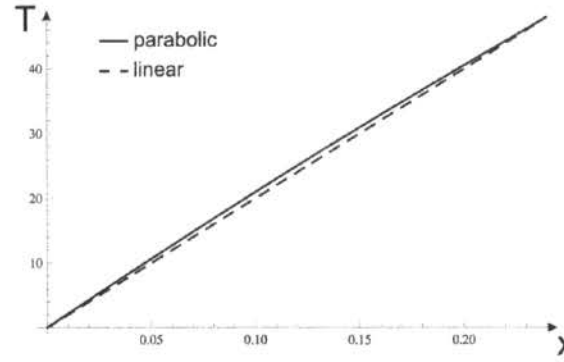

Figure 5. Ten-element patch test. Linear and parabolic temperature fields, eqs. (8) for $y = 0$, and (9).

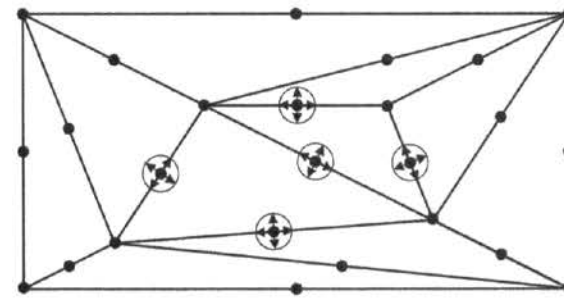

Figure 6. Ten-element patch test. Shifted nodes to obtain distorted meshes.

obtained by adding a parabolic function with the maximum equal to 1 to the linear field $200x$, see Fig. 5.

The values of temperature calculated by the above formulae are imposed at the external nodes (1,...,8) while at the internal nodes (9,...,25) we check the computed values; they must agree with these yielded by either eq. (8) or (9). The thermal conductivity $k = 1.0$.

Typically, this test is performed for the regular mesh of Fig. 4, but we also check 2 cases of distorted meshes, with the side nodes 21,...,25 shifted as follows: (1) in the directions along the sides, and (2) in an arbitrary direction, see Fig. 6. The positions of the shifted nodes are independently randomly generated 1000 times and a run is performed for each distorted mesh in order to preclude passing this test accidently for a particular combination of shifts. The shift of the node is a pseudo-random real number generated in the range $[-r, r]$, where $r = 0.008$.

Table 1. Patch test. Maximum relative error of eq. (10) (%).

Element	Regular mesh	Distorted mesh, shift: along the side	arbitrary
Linear temperature of eq. (8)			
3, 6, 6c	0	0	0
4, 8, 8c, 9, 9c	0	0	0
Parabolic temperature of eq. (9)			
3	3.28897	3.37994	3.46666
6	2.22257	2.24071	2.26558
6c	2.22257	2.22351	2.24721
8	1.46792	1.75862	1.78442
8c	1.46792	1.46792	1.63673
9	2.05298	2.08153	2.10083
9c	2.05298	2.05298	2.05719
4	3.39125	3.39847	3.42160

First, for each run, we compute the *max*-norm in R^n for each component over the internal nodes I. This norm is defined as $T \doteq \|T\|_\infty = \max |T_I|$, where $\max |T_I| = \max T_I$ as $T_I \geq 0$. Next, the relative error for a particular run is computed using this norm and the analytical solution T_{ana} obtained by eq. (8) or eq. (9). The final formula for the error is as follows

$$e \doteq \max \frac{Abs(T_{ana} - T)}{T_{ana}} \times 100\% \geq 0, \tag{10}$$

where the maximum is computed over all runs. The results are presented in Table 1, and we see that

1. for the linear temperature field, all the tested elements yield zero errors, which means that they pass the patch test also for shifted nodes. Note that this result differs from that obtained for the 9-node elements based on the two-level interpolation schemes, i.e. MITC9i in (Wisniewski & Panasz 2013) and the other 9-node elements in (Panasz, Wisniewski, & Turska 2013).
2. for the parabolic temperature field, all the tested 6-node elements yield nonzero errors for shifted nodes, which means that they fail this test. However, the element with the corrected shape functions "6c" is more accurate in all cases than the standard element "6". Besides, the shifts along the edge yield smaller errors than the shifts in arbitrary directions.

3.3 *Radial conduction problem*

In this problem, temperature varies only with the radial coordinate r and the effect of shifting the side nodes of triangular elements in the radial direction is examined.

The finite element mesh and the boundary conditions are shown in Fig. 7, where the inner radius $r_i = 1$, the outer radius $r_o = 256$, and $\Delta r_2 = 63.75$. The values of temperature prescribed at the inner and the outer boundary are $T_i = r_i$ and $T_o = r_o$, respectively. The thermal conductivity $k = 1$. The analytic solution

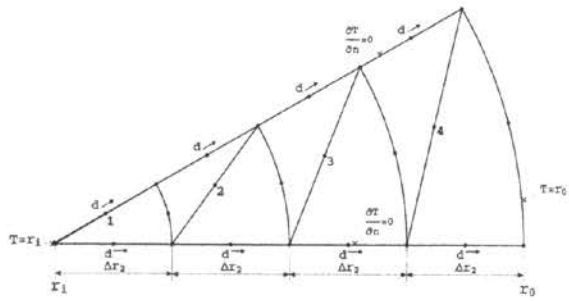

Figure 7. Radial conduction problem. Finite element mesh and boundary conditions. Positive direction of shift d is shown.

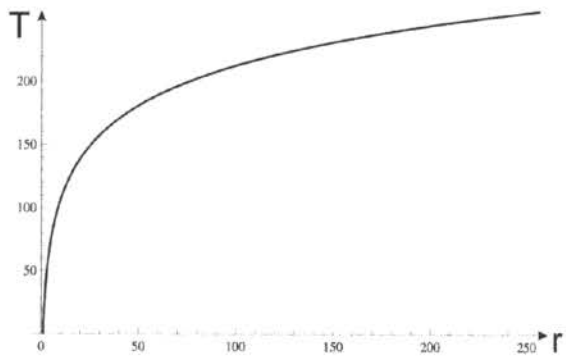

Figure 8. Radial conduction. Analytic solution of eq. (11).

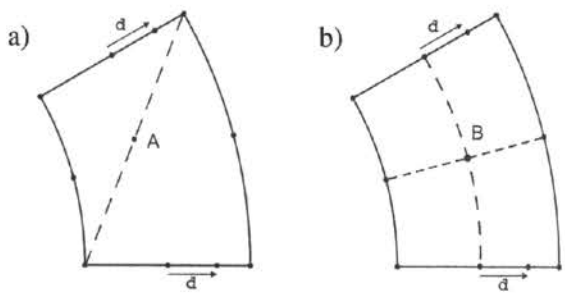

Figure 9. Radial conduction. Two positions of 'central' node: (a) at the middle of a diagonal, (b) at the middle of an arc.

is as follows:

$$T_{ana} = \frac{T_i \ln(\frac{r_o}{r}) + T_o \ln(\frac{r}{r_i})}{\ln(\frac{r_o}{r_i})}, \tag{11}$$

see (Carslaw & Jaeger 1989, p. 189). It is plotted in Fig. 8 and we see that it is highly nonlinear.

This problem is solved in (Celia & Gray 1984) using the 8-node elements based on the standard and the corrected shape functions and 4×4 Gauss integration. We divide each of the 8-node elements into two 6-node triangular elements, and locate the additional 'central' nodes (1,...,4) either at the middle of a diagonal (position A) or at the middle of an arc (position B), see Fig. 9. Positions of the 'central' nodes are fixed when the side-nodes are shifted.

The distorted meshes are obtained by shifting the side-nodes of the triangles in the radial direction by

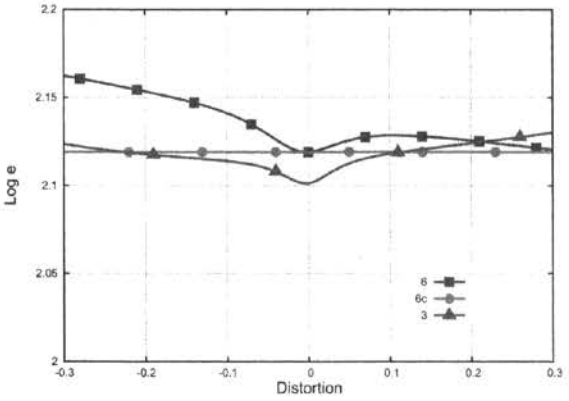

Figure 10. Radial conduction. Error for triangular elements. 'Central' nodes A.

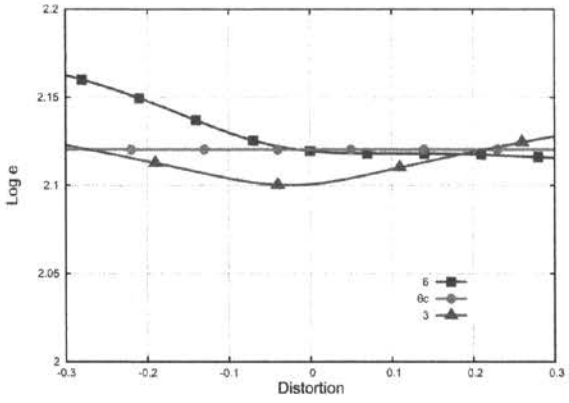

Figure 11. Radial conduction. Error for triangular elements. 'Central' nodes B.

$d \in [-0.3, 0.3]$. Totally, 61 meshes are used, for the values of d differing by 0.01. The solution error is calculated as in (Celia & Gray 1984),

$$e(d) \doteq \left\{ \frac{1}{L} \int_{r_i}^{r_o} [T_{ana} - T(d)]^2 \, dr \right\}^{1/2} \geq 0, \qquad (12)$$

where $T(d)$ is the FE solution for a distorted mesh.

The plots of errors for triangular elements as functions of d, for both positions of the 'central' nodes, are presented in Figs. 10 and 11, while for quadrilateral elements in Figs. 12 and 13.

Besides, the average logarithmic error $\log_{10} e(d)$ computed over the whole range of $d \in [-0.25, 0.25]$ is presented in Table 2. The range of d is narrowed to compare to the results of (Celia & Gray 1984), Fig. 7, which go to infinity for larger values of d.

The results obtained can be summarized as follows:

1. The triangular 6-node elements based on the corrected shape functions are practically insensitive to distortions, as the error remains constant regardless of d. They do not fail for large distortions ($|d| > 0.3$) differently than the elements based on the standard shape functions. Similarly behave 8- and 9-node elements using the corrected shape functions.

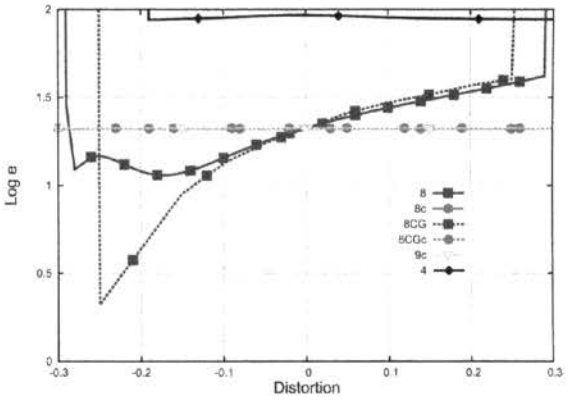

Figure 12. Radial conduction. Error for quadrilateral elements. 'Central' nodes A.

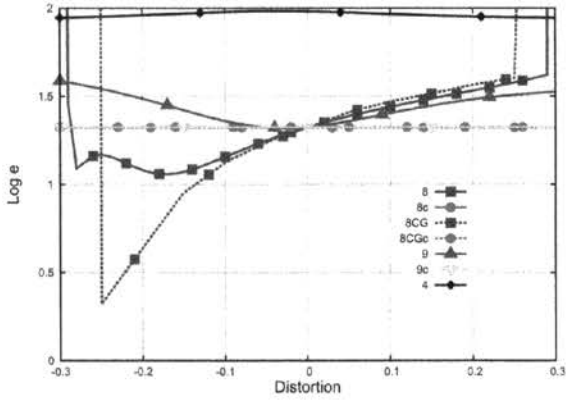

Figure 13. Radial conduction. Error for quadrilateral elements. 'Central' nodes B.

Table 2. Radial conduction. Logarithmic average error $\log_{10} e$ for $d \in [-0.25, 0.25]$.

	Position of 'central' node	
Element	A	B
6	2.13418	2.12711
6c	2.11904	2.12036
3	2.11574	2.10940
8	1.31058	1.31058
8c	1.32478	1.32478
8CG	1.20758	1.20758
8CGc	1.322	1.322
9	-[1]	1.41295
9c	1.32476	1.32476
4	1.9542[2]	1.96812

[1]Negative Jacobian at Gauss point encountered
[2]For "4" error was computed for $d \in (-0.20, 0.25]$

2. The order of average errors for triangular elements is almost 1 order higher than for quadrilateral elements, which can be linked to the number of Gauss points; only 3 in the case of 6-node triangles and 16 in the case of 8-node quadrilaterals of (Celia & Gray 1984) and 9 in the case of ours 9-node elements.

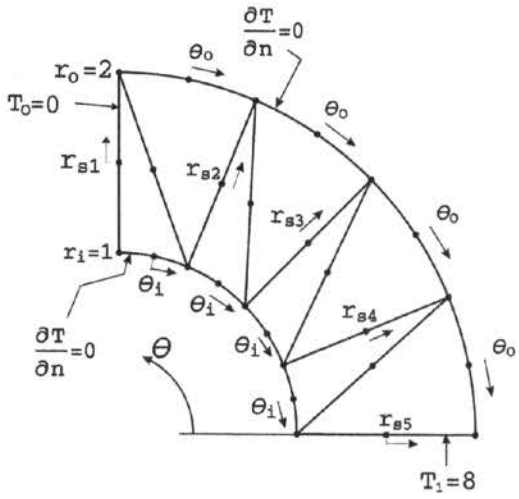

Figure 14. Angular conduction. Finite element mesh and boundary conditions.

3. The level of errors shown by all triangular elements is similar, although small differences can be noticed, and "6c" is more accurate than "6". The difference between the results for both positions of the 'central' nodes is small.
4. A very strong sensitivity of the quadrilateral element based on the standard shape functions of (Celia & Gray 1984) to distortions is not shown by our 8- and 9-node elements; compare the curves "8CG", "8" and "9" in Figs. 12 and 13. It is likely that this sensitivity of "8CG" is caused by the single precision used in calculations.

3.4 *Angular conduction problem*

In this example temperature varies with the angle θ and the effect of shifting of the side nodes of triangular elements is examined.

The finite element mesh and the boundary conditions are shown in Fig. 14; the temperate values are prescribed only at the straight edges. The thermal conductivity $k = 1$.

This problem is solved in (Celia & Gray 1984) using the 8-node elements based on the standard and the corrected shape functions and 4×4 Gauss integration. We divide each of the 8-node elements into two 6-node triangular elements and locate the additional node at the middle of a diagonal.

To change positions of side nodes of the triangular elements, we perturb either (a) the radial coordinates r_{si}, or (b) the angular coordinates of the inner and outer boundaries, θ_i and θ_o, respectively, see Fig. 14.

The solution error is defined as follows:

$$e(d) \doteq \left(\frac{1}{n} \sum_{k}^{n} e_k^2(d) \right)^{1/2} \geq 0, \quad e_k(d) \doteq T_{ana} - T_k(d), \quad (13)$$

where $T_k(d)$ is the FE solution at node k and n is the number of nodes where temperature is computed. The analytic solution is

$$T_{ana} = (T_0 - T_1)\frac{2\theta}{\pi} + T_1, \qquad 0 \leq \theta \leq \frac{\theta}{2}, \qquad (14)$$

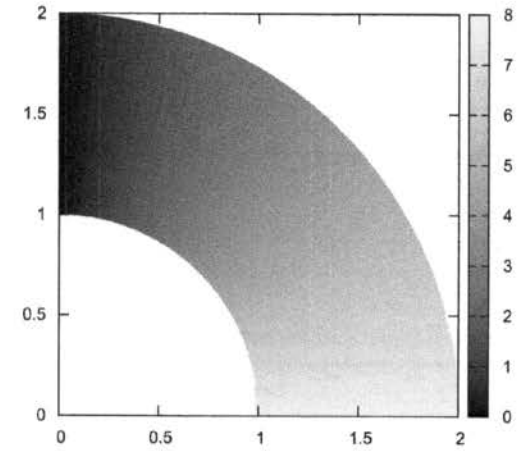

Figure 15. Angular conduction. Analytic solution of eq. (14).

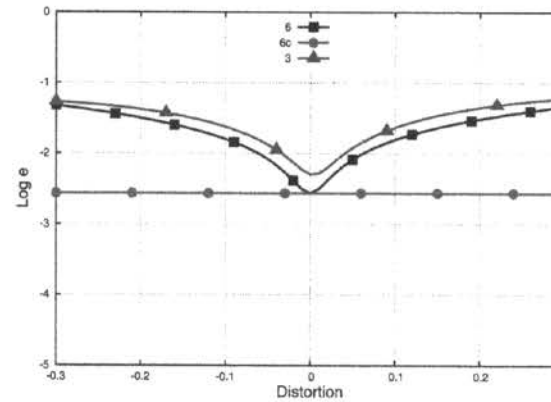

Figure 16. Angular conduction. Error for triangular elements. Distortion 1.

see Fig. 15. Two cases of mesh distortions are tested:

1. The radial coordinates are changed as follows: $r_{s1}, r_{s3}, r_{s5} = d$ and $r_{s2}, r_{s4} = -d$, i.e. identically but in opposite directions. The angular coordinates θ_o and θ_i remain unchanged.
2. The angular coordinates are changed as follows: $\Delta\theta_o = d$ and $\Delta\theta_i = -d$, where the nodes at θ_o are moved clockwise and those at θ_i counterclockwise. The radial coordinates r_{si} are unchanged.

The plots of errors for triangular elements as functions of d are shown in Figs. 16 and 17, while for quadrilateral elements in Figs. 18 and 19. The logarithmic average error $\log_{10} e(d)$ computed over the whole range of distortions is presented in Table 3.

The results obtained can be concluded as follows:

1. The triangular 6-node elements based on the corrected shape functions are insensitive to distortions. They do not fail for large distortions ($|d| > 0.3$) differently from the elements based on the standard shape functions. This is similar to the behavior of 8- and 9-node elements using the corrected shape functions.

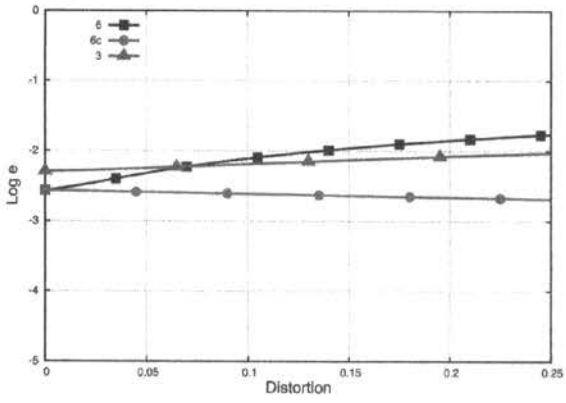

Figure 17. Angular conduction. Error for triangular elements. Distortion 2.

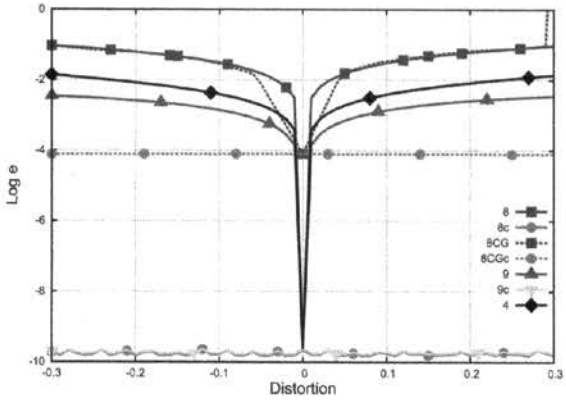

Figure 18. Angular conduction. Error for quadrilateral elements. Distortion 1.

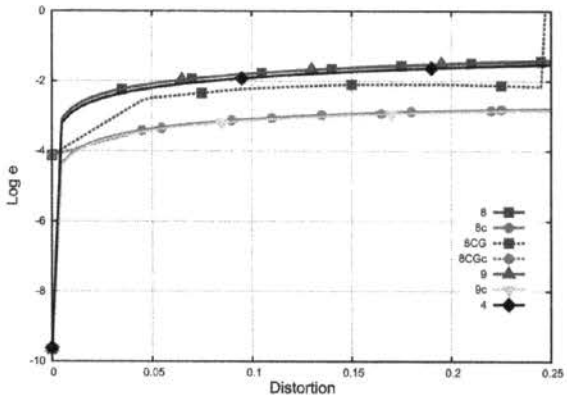

Figure 19. Angular conduction. Error for quadrilateral elements. Distortion 2.

2. Comparing the level of errors for triangular elements we see that "6c" is always more accurate than "6". The average errors for triangular elements are always higher than for quadrilateral elements, and for the distortions 1 the difference is about 7 orders!
3. Our 8- and 9-node elements are not so strongly sensitive to distortions as the quadrilateral element based on the standard shape functions of (Celia & Gray 1984); compare the elements "8", "9" and "8CG" in Fig. 18. Besides, the error for "8CGc" of (Celia & Gray 1984) and our "8c" also is very different, which is probably caused by the difference in the precision of calculations, single in the cited paper and double in ours.

Table 3. Angular conduction. Logarithmic average error $\log_{10} e(d)$.

	Distortion cases	
Element	1	2
6	−1.71925	−2.07996
6c	−2.56305	−2.62282
3	−1.56278	−2.15933
8	−1.56620	−1.96007
8c	−9.76461	−3.24304
8CG	−1.52027	−2.31170
8CGc	−4.10353	−3.15025
9	−2.90955	−1.95100
9c	−9.72801	−3.28543
4	−2.42641	−2.06517

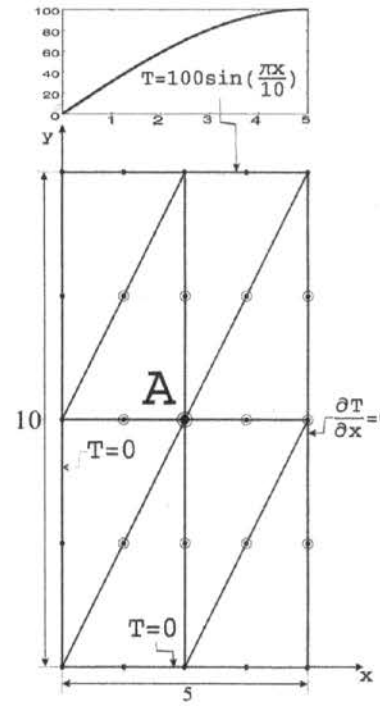

Figure 20. Two-dimensional conduction. Mesh and boundary conditions.

3.5 *Two-dimensional conduction problem*

In this test the analyzed area is rectangular and the effect of shifting the central node A is examined. The finite element mesh and the boundary conditions are shown in Fig. 20, the thermal conductivity $k = 1$. The exact solution is

$$T_{ana}(x, y) \doteq 100 \frac{\sinh(\frac{\pi y}{10}) \sin(\frac{\pi x}{10})}{\sinh \pi}, \qquad (15)$$

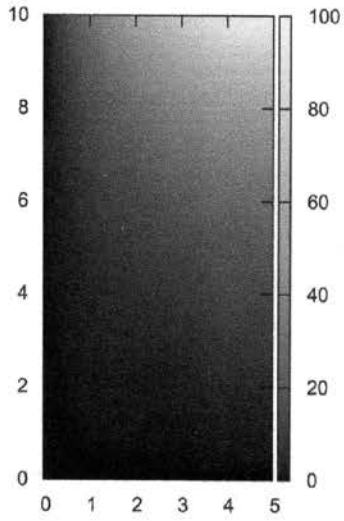

Figure 21. Two-dimensional conduction. Exact solution of eq. (15).

Table 4. Two-dimensional conduction. Comparison of our triangular elements and the control volume elements of (Charoensuk & Vessakosol 2010). Non-distorted mesh.

Element	Error (%)
6c	1.016
6v	1.074
3	4.235
3v	4.235

see Fig. 21. The average error of the temperature field is calculated as follows:

$$e(d) \doteq \frac{1}{n}\sum_{i=1}^{n}\left|\frac{T_{ana}-T(d)}{T_{ana}}\right| \times 100\%, \qquad (16)$$

where $T(d)$ is the FE solution and n is the number of nodes.

The errors for the regular non-distorted mesh for our "6c" and "3" elements and the control volume elements "6v" and "3v" of (Charoensuk & Vessakosol 2010) are shown in Table 4.

The distorted mesh is obtained for two types of shifts of the central node A: (1) along the diagonal and (2) perpendicularly to the diagonal. The plots of errors as a function of $d \in (-0.1, +0.1)$ for triangular elements are shown in Figs. 22 and 23 while for quadrilateral elements in Figs. 24 and 25. The error of eq. (16) for triangular and quadrilateral elements and both distorted meshes is given in Table 5.

The obtained results lead us to the following conclusions:

1. The triangular 6-node element based on the corrected shape functions "6c" is more accurate than the element based on the standard shape functions "6".

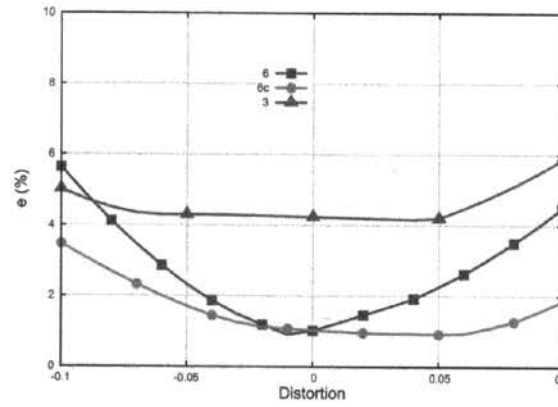

Figure 22. Two-dimensional conduction. Error for triangular elements. Shift of node A along the diagonal.

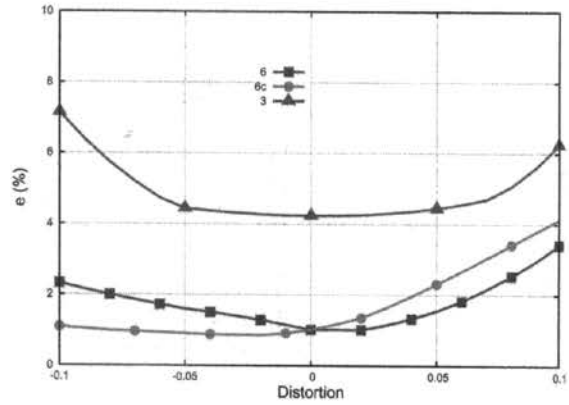

Figure 23. Two-dimensional conduction. Error for triangular elements. Shift perpendicular to the diagonal.

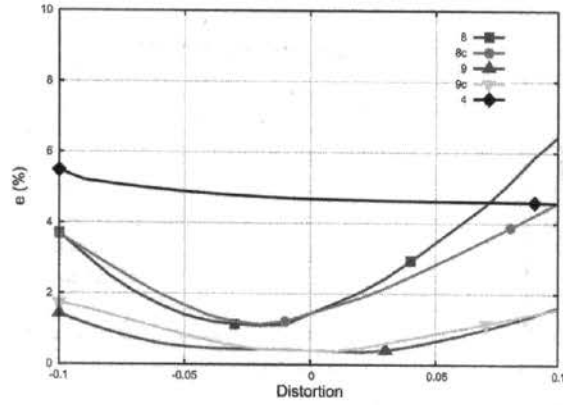

Figure 24. Two-dimensional conduction. Error for quadrilateral elements. Shift of node A along the diagonal.

2. For the non-distorted mesh, our element "6c" is slightly more accurate than the control volume element "6v", while the 3-node elements "3" and "3v" have an identical accuracy, also nodewise. For the distorted mesh, the average errors for triangular elements are higher than for quadrilateral 9-node elements and lower than for 8-node elements.
3. The 9-node elements are more accurate than 8-node elements despite fewer Gauss points,

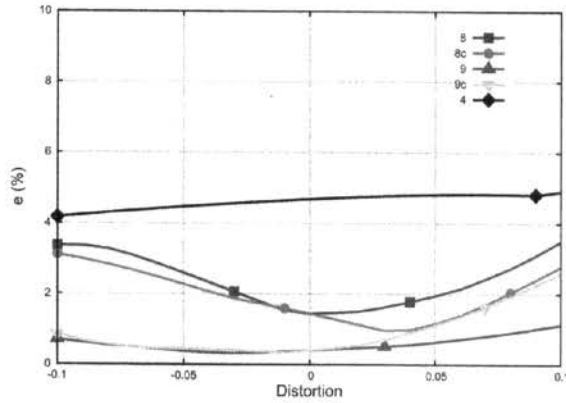

Figure 25. Two-dimensional conduction. Error for quadrilateral elements. Shift perpendicular to the diagonal.

Table 5. Two-dimensional conduction. Error (%) for triangular and quadrilateral elements. Distorted mesh.

	Distortion. Shift of A:	
Elements	along diagonal	perpendicular to diagonal
6	2.66181	1.76076
6c	1.55317	1.71238
3	4.53207	4.89751
8	2.81351	2.37502
8c	2.50368	1.94347
9	0.75438	0.57428
9c	0.94083	0.89630
4	4.79235	4.62029

however, the corrected shape functions are not beneficial for them and the error defined by eq. (16) of "9c" is bigger than of "9".

4 FINAL REMARKS

In the current paper, the corrected shape functions were formulated in terms of the area (barycentric) coordinates and used, instead of the standard isoparametric ones, in the two-dimensional six-node element for heat conduction. The basic features of the new element are as follows:

1. it has a correct number of zero eigenvalues (1) for regular and distorted meshes. The element shapes implied by the corrected shape functions are more regular than these by the standard shape functions, so the negative areas are less likely to appear. The 3-point Gauss integration suffices to ensure nonnegative eigenvalues.
2. it passes the patch test for the linear temperature field for regular and distorted meshes. For the parabolic temperature field, the new element is more accurate than the element based on the standard shape functions.

The new element was subjected to the tests including the radial, angular and two-dimensional conduction and its accuracy was compared to several other triangular and quadrilateral elements for various mesh distortions; the detailed conclusions are given in Sects. 3.3–3.5. Generally, we can say that the new element is more accurate and less sensitive to mesh distortions than the standard one. Hence, the corrected shape functions are worthwhile implementing.

REFERENCES

Carslaw, H. & J. Jaeger (1989). *Conduction of heat in solids.* Clarendon Press.

Celia, M. & W. Gray (1984). An improved isoparametric transformation for finite element analysis. *Int. J. Num. Meth. Engng 20*, 1447–1459.

Charoensuk, J. & P. Vessakosol (2010). A high order control volume finite element procedure for transient heat conduction analysis of functionally graded materials. *Heat and Mass Transfer 46*, 1261–1276.

Irons, B. (1966). Numerical integration applied to finite element methods. *Proc. Conf. on Use of Digital Computers in Structural Engineering*.

Panasz, P., K. Wisniewski, & E. Turska (2013). Reduction of mesh distortion effects for nine-node elements using corrected shape functions. *Finite Element in Analysis and Design 66*, 83–95.

Simulia (2010). *ABAQUS*. Ver.6.10-2.

Taylor, R. (2010). *Program FEAP*. Ver.8.3. University of California at Berkeley.

Wisniewski, K. & P. Panasz (2013). Two improvements in formulation of nine-node element mitc 9. *Int. J. Num. Meth. Engng 93*, 612–634.

Zienkiewicz, O., R. Taylor, & J. Zhu (2005). *The Finite Element Method. Sixth Edition. Vol.1. Its Basis and Fundamentals*. Elsevier.